TOPICAL REVIEW • OPEN ACCESS

Manipulating magnetism by ultrafast control of the exchange interaction

To cite this article: J H Mentink 2017 *J. Phys.: Condens. Matter* **29** 453001

View the article online for updates and enhancements.

Topical Review

Manipulating magnetism by ultrafast control of the exchange interaction

J H Mentink

Radboud University Nijmegen, Institute for Molecules and Materials, Heijendaalseweg 135, 6525 AJ, Nijmegen, Netherlands

E-mail: J.Mentink@science.ru.nl

CrossMark

Abstract

In recent years, the optical control of exchange interactions has emerged as an exciting new direction in the study of the ultrafast optical control of magnetic order. Here we review recent theoretical works on antiferromagnetic systems, devoted to (i) simulating the ultrafast control of exchange interactions, (ii) modeling the strongly nonequilibrium response of the magnetic order and (iii) the relation with relevant experimental works developed in parallel. In addition to the excitation of spin precession, we discuss examples of rapid cooling and the control of ultrafast coherent longitudinal spin dynamics in response to femtosecond optically induced perturbations of exchange interactions. These elucidate the potential for exploiting the control of exchange interactions to find new scenarios for both faster and more energy-efficient manipulation of magnetism.

Keywords: exchange interactions, ultrafast magnetism, strongly correlated electrons

(Some figures may appear in colour only in the online journal)

1. Introduction

Ordering of microscopic spins in magnetic materials originates from the exchange interaction J_{ex}, the strongest interaction in magnetism, which exceeds the strength of external magnetic fields by orders of magnitude. On a fundamental level, exchange interactions emerge from the repulsive Coulomb interactions between electrons and are most sensitive to electronic perturbations. This fact implies intriguing possibilities for the ultrafast control of magnetism by femtosecond laser pulses, which is a very active research field initiated two decades ago with the ground breaking discovery of sub-picosecond demagnetization of ferromagnetic Ni by a 60 femtosecond laser pulse [1] and the observation of laser-induced ferromagnetic [2] and antiferromagnetic resonance [3], followed by the observation of all-optical switching in ferrimagnetic GdFeCo alloys [4–7] and subsequently the highly intriguing observation of distinct dynamics between exchange coupled spins in different magnetic sublattices [8–10]. Moreover, a further stimulus to the field was given by the demonstration of helicity dependent all-optical switching in ferromagnetic multilayers [11], which are materials of great interest for magnetic data storage and, very recently, by the demonstration of all-optical magnetic recording in transparent ferrimagnetic oxides [12], enabling magnetic recording that is both ultrafast and takes place at unprecedentedly low heat load.

All the above experiments can be understood by accounting for (a combination of) laser-induced heating, generation of effective opto-magnetic fields and/or optical perturbations to the magnetic anisotropy, but do not directly provide indications for time-dependent exchange interactions. Interestingly, however, considerable experimental evidence has been has been presented as well for dynamical exchange effects,
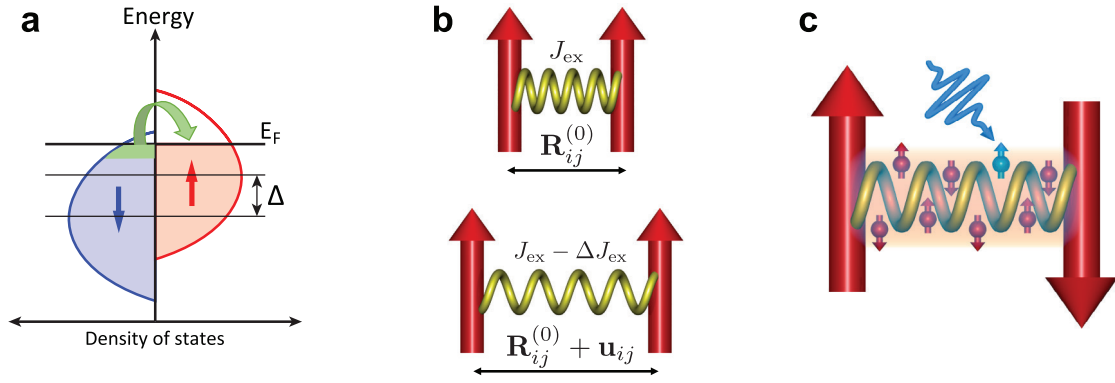
Figure 1. Illustrated examples of the effect of laser excitation on exchange effects in magnetic systems. (a) Collapse of the exchange splitting in itinerant ferromagnets as a result of the redistribution of laser-excited electrons between the majority and minority band (green arrow). (b) optical excitation of phonons change the positions of the atomic nuclei R_{ij}, leading to a perturbation of the exchange interaction (yellow spirals) between spins localized around the different nuclei (red arrows). (c) femtosecond laser excitation (blue pulse) of electrons (small spheres with arrows) can change both the band structure and the electronic distribution. This yields perturbations to the exchange interaction (glowing yellow spiral) between spins localized at different sites (big red arrows). Case (c) is the focus of this review.

including a collapse of the exchange splitting in Ni, Gd and Co metals [13–16] (illustrated in figure 1(a)), modulation of J_{ex} by excitation of an optical phonon at the Gd metal surface [17] (figure 1(b)), laser-induced heating across the antiferromagnetic-ferromagnetic transition in FeRh [18, 19] and, more recently, detection of the dynamics of the exchange energy [20], as well as triggering both coherent macroscopic spin precession [21] and longitudinal oscillation of the order parameter in magnetic insulators [22] by optical perturbations of J_{ex} (figure 1(c)). Furthermore, the ability to control the exchange interaction by time-dependent electric fields has intrigued researchers in several other areas of physics, including quantum computing based on semiconductor quantum dots [23–25], ultracold atoms [26–28], strongly correlated materials [29–31] and semiconductors doped with impurity spins [32–37].

Despite this significant amount of studies, the problem of understanding and modeling how magnetism can be manipulated by ultrafast control of exchange interactions is still far from being solved. In particular, while considerable progress has been made for describing optical control of J_{ex} in one and two spin systems [23–26] the generalization to extended magnetically ordered systems is non-trivial as it requires to understand how laser pulses influence both the band structure and the electronic correlations. This is a highly challenging problem, since it implies the solution of a strongly time-dependent quantum many-body problem of an extended system. Moreover, when exchange interactions are perturbed on time scales much shorter than the equilibration of the magnetic system, the latter can be brought in a strongly nonequilibrium state which cannot be treated within a conventional thermodynamical approach. Even in the semi-classical regime, where spins can be treated as classical vectors, simulating the time-dependent response of the macroscopic magnetic order to ultrafast modifications of atomic-scale exchange interactions defines a challenging multi-scale problem.

Early works addressing both the optical control of exchange interactions and the response of magnetic order focused on ferromagnets, in particular ferromagnetic semiconductors

[35]. However, in ferromagnetic systems the excitation of spin dynamics requires a change of the total angular momentum. This makes it difficult to induce fast dynamics by modifying J_{ex}. Antiferromagnetic (AFM) systems do not suffer from this bottleneck and therefore provide novel opportunities to manipulate the dynamics of magnetic order by ultrafast control of J_{ex}. This review article provides an overview of the recent developments for modeling such antiferromagnetic systems [21, 22, 38–40] and is organized as follows. First, we introduce various analytical methods that enable the definition of exchange interactions under electronic nonequilibrium conditions and outline the computational methods used to evaluate the resulting formulas. Second, results on the ultrafast control of J_{ex} are discussed using the single-band Mott-Hubbard insulator at half-filling as a model system, which allows to study both resonant electronic excitations as well as non-resonant periodic driving. Third, the manipulation of magnetic order by the ultrafast control of exchange interactions is discussed, focusing on four examples: (a) the excitation of macroscopic spin precession in canted antiferromagnets, (b) cooling of antiferromagnetically ordered classical spins (c) excitation of coherent longitudinal oscillations of the AFM order parameter, and (d) effective time reversal in quantum spin chains. Finally, we draw conclusions and discuss several directions for further research.

2. Methods of computing time-dependent exchange interactions

Most of the calculations on the ultrafast control of J_{ex} reported here are based on calculations using the paradigm single band Hubbard model. The advantage of using the single band Hubbard model is that J_{ex} in equilibrium is very well understood and serves as minimal model for describing exchange interactions in magnetic oxides. At the same time, recently established computational techniques can be exploited to study the nonequilibrium electron dynamics for extended systems, enabling the evaluation of J_{ex} out of equilibrium. Below we start by briefly introducing the Hubbard model and

subsequently outline the methods used to solve it out of equilibrium. Finally, we introduce three distinct methods to evaluate J_{ex} under electronic nonequilibrium conditions.

2.1. Hubbard model

The Hamiltonian of the Hubbard model is given by

$$H = -t_0 \sum_{\langle ij \rangle \sigma} c_{i\sigma}^\dagger c_{j\sigma} + U \sum_j n_{j\uparrow} n_{j\downarrow}. \qquad (1)$$

Here $c_{i\sigma}^\dagger$ creates an electron at site i with spin $\sigma = \uparrow, \downarrow$, t_0 is the hopping between nearest-neighbor sites and U the repulsive on-site interaction U. For half-filling and at $U/t_0 \gg 1$ this model describes a Mott-insulator with one electron per site. The AFM exchange coupling between the spin degrees of freedom follows from the well-known kinetic exchange mechanism [41], where the system gains energy by virtual hoppings to adjacent sites. Due to the Pauli principle, such hoppings are only possible when adjacent sites have opposite spin. A simple perturbative calculation in t_0 shows that the spin degrees of freedom are described by an AFM Heisenberg Hamiltonian $H_{ex} = J_{ex} \sum_{ij} \mathbf{S}_i \cdot \mathbf{S}_j$, where $J_{ex} = 2t_0^2/U$ is the exchange interaction (see also figure 3(a)), which has been derived more rigorously based on a canonical transformation technique [42–45].

For the evaluation of J_{ex} below, it is convenient to include also a homogenous static magnetic field described by

$$H_Z = B_x \sum_j S_{jx}. \qquad (2)$$

where the spin $S_{j\alpha} = \frac{1}{2} \sum_{\sigma\sigma'} c_{j\sigma}^\dagger (\hat{\sigma}_\alpha)_{\sigma\sigma'} c_{j\sigma'}$ is coupled to a homogeneous magnetic field B_x along the x axis ($\alpha = x, y, z$; $\hat{\sigma}_\alpha$ denote the Pauli matrices). Non-equilibrium dynamics due to time-dependent electric fields $\mathbf{E}(t)$ can be most conveniently incorporated by including a Peierls phase [46, 47] to the hopping:

$$t_{ij}(t) = t_0 \exp \left[i e \mathbf{A}(t) \cdot (\mathbf{R}_i - \mathbf{R}_j)/\hbar \right], \qquad (3)$$

where $\mathbf{A}(t) = -\partial_t \mathbf{E}(t)$ is the homogenous vector potential. Physically, this is equivalent to using a gauge in which the electric field is included by adding a scalar potential at each site, $e\phi_i(t) \sim \mathbf{R}_i \cdot \mathbf{E}(t)$.

To solve the Hubbard model in the presence of time-dependent electric fields, we outline two complementary methods used to obtain the results discussed in this review. First, the nonequilibrium extension of the dynamical mean field theory (DMFT), which enables the investigation of magnetically ordered systems directly in the thermodynamic limit. Second, direct simulation of the time-dependent Schrödinger equation using exact diagonalization for finite size one-dimensional systems.

The implementation of nonequilibrium DMFT was reviewed in detail in [48]. In short, within DMFT [49] the problem of interacting electrons on a lattice is mapped onto the solution of an effective single-site impurity coupled to a non-interacting bath, that is determined self-consistently. This
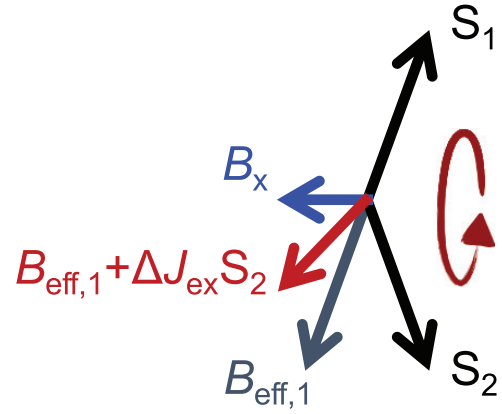

Figure 2. Evaluation of the nonequilibrium $J_{ex}(t)$ in a canted antiferromagnet. In equilibrium, the effective field $B_{eff,1}$ (grey arrow) is antiparallel to the sublattice magnetization $\mathbf{S}_1$ (upper black arrow). A modification of the exchange interaction (ΔJ_{ex}) would rotate the effective field (red arrow) with respect to $\mathbf{S}_1$ causing the excitation of a spin resonance. In turn, $\Delta J_{ex}(t)$ can be inferred from the observed spin precession.

results in a mean field theory for the spatial degrees of freedom while keeping temporal correlations and was shown to be the exact solution of the Hubbard model in the limit of infinite dimensions [50]. For the nonequilibrium case, the model can be solved using the perturbative hybridization expansion (non-crossing approximation [51]), which at large U shows good agreement with more accurate impurity solvers. Further, to solve the Hubbard model in the presence of a transverse magnetic field, spin-flip terms were included in the solution of the impurity model. The detailed implementation for the hypercubic lattice is described in [38].

Exact diagonalization solves directly the Schrödinger equation with the time-dependent Hamiltonian $H(t)$ from a given initial state $|\psi_0\rangle$. For systems of a few sites, evaluation of the time propagator $\exp(-iH(t)/\hbar)$ can be done directly by numerically diagonalizing $H(t)$. For larger systems, a more efficient scheme is required and the Krylov technique was used [52]. In both cases, this is combined with a commutator-free exponential time-propagation scheme [53]. Being related to the Magnus expansion, it preserves unitarity and yields a high-order accurate time integration of the Schrödinger equation.

2.2. Nonequilbrium exchange in canted antiferromagnets

A simple instrumental way to evaluate a nonequilibrium exchange interaction is by studying a two-sublattice antiferromagnet canted by an external magnetic field [38]. In the regime where a rigid macrospin model would be valid, the dynamics of the sublattice macrospin is governed by the Landau-Lifshitz equation

$$\hbar \partial_t \langle \mathbf{S}_1 \rangle = -\langle \mathbf{S}_1 \rangle \times (B_x \mathbf{e}_x - 2J_{ex} \langle \mathbf{S}_2 \rangle), \qquad (4)$$

where $\langle \mathbf{S}_{1,2} \rangle$ is the macrospin on sublattice 1, 2; J_{ex} is the effective exchange interaction and B_x is the strength of the transverse magnetic field. With $\langle \mathbf{S}_{1,2}(t) \rangle$ given from the solution of the full electronic model, the effective exchange interactions
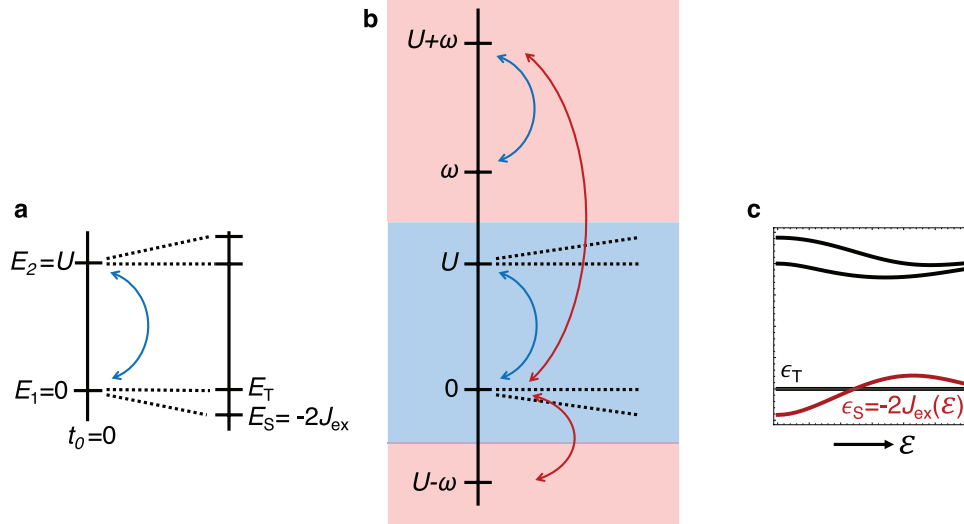
Figure 3. Floquet theory of nonequilibrium J_{ex} in a two-site Hubbard model. (a) In the atomic limit, there are four states. Two of them ($|\uparrow,\downarrow\rangle$ and $|\downarrow,\uparrow\rangle$) are singly occupied sites at $E_1 = 0$ while the other two states involve a doubly occupied and empty site at energy $E_2 = U$ ($|\uparrow\downarrow, 0\rangle$ and $|0,\uparrow\downarrow\rangle$). Due to virtual hoppings between these sets of states (blue arrows, the degeneracy is lifted and the lowest states become singlet and triplet states at energies $E_S = -2J_{ex}$ and $E_T = 0$, respectively). (b) In the presence of a time-periodic field, there are also virtual hoppings induced by absorption and emission of photons (red arrows), coupling different Floquet sectors (red and blue panels). (c) Floquet spectrum as function of driving amplitude $\mathcal{E}$. The exchange interaction is extracted from the amplitude dependent singlet-triplet splitting $\epsilon_T - \epsilon_S$.

can be inferred from inverting equation (4). Using Néel symmetry, $\langle S_{1y,z}\rangle = -\langle S_{2y,z}\rangle$, $\langle S_{1x}\rangle = +\langle S_{2x}\rangle$ one obtains

$$J_{ex}(t) = -\frac{B_x}{4\langle S_{1x}\rangle} - \frac{1}{4\langle S_{1x}\rangle}\frac{\hbar\partial_t\langle S_{1y}\rangle}{\langle S_{1z}\rangle}. \tag{5}$$

This result can be interpreted as follows. The first term on the right gives the equilibrium value of J_{ex} which is determined by the canting induced by B_x. As illustrated in figure 2, in this case the effective field $\mathbf{B}_1 = B_x\mathbf{e}_x - 2J_{ex}\langle S_2\rangle$ is parallel to $\langle S_1\rangle$ and no dynamics occurs. If however, J_{ex} is suddenly perturbed by an amount ΔJ_{ex}, the effective field is no longer collinear to $\langle S_1\rangle$ and a precession is triggered, leading to the appearance of the second term in equation (5). While this interpretation may seem conceptually attractive, we stress that the validity of the instantanous approximation used in the derivation of equation (4) is a fundamental question which in general has not been solved (see also the discussion in [38]). For the purpose of this review, we regard equation (5) as the best estimate of an instantaneous J_{ex} that is in accordance with an observed macrospin dynamics.

2.3. General formulas for nonequilibrium exchange

Instead of explicitly simulating the full electron dynamics in the canted geometry, it is also possible to derive explicit formulas for the response to small rotations of spins. In equilibrium, this approach was introduced by Lichtenstein, Katsnelson and coworkers [54–57]. For two spin moments at site i and j rotated by a small angle $\pm\theta/2$ the relative energy change can be written as $\delta E_{ij} \approx \frac{1}{2}J_{ij}\theta^2$. In the single band Hubbard model the pair-interactions than become [57]

$$J_{ij} = -\mathrm{Tr}_E\left(\Sigma_i^s(E)G_{ij}^\uparrow(E)\Sigma_j^s(E)G_{ji}^\downarrow(E)\right). \tag{6}$$

Here $\Sigma_i^s(E) = \left(\Sigma_i^\uparrow(E) - E_i^\downarrow(\omega)\right)/2$ is the spin-dependent part of the self-energy which is taken only locally at site i. $G_{ij}^\sigma(E)$ is the spin-dependent single-particle Green's function and the trace is over all electron energies E. It is useful to realize that already this equilibrium result indicates a profound difference between the exchange splitting observed in photo-emission experiments and the intersite exchange interaction J_{ij} responsible for ordering of spin moments. While in simplest approximation the exchange splitting is determined $\Sigma_i^s(0)$ (Stoner model), the J_{ij}'s are also dependent on the Green's function and hence even in equilibrium it is not possible to directly extract intersite exchange interactions from photo-emission data.

The concept of rotating local moments can be generalized also to the time-dependent case [58]. In this case, an effective spin action is defined in terms of time dependent rotations of the spin quantization axes $\mathbf{e}_i(t)$, as described by Holstein–Primakoff bosons $\xi_i(t)$. Starting from the electronic partition function as a path integral over fermionic fields ϕ, one introduces rotated fermion fields ψ and then expands the action to second order in ξ. The rotated fermionic fields are integrated out, which leads to spin action with an interaction term of the form $\mathcal{S}_{spin}[\xi^*, \xi] = \sum_{ij}\int dt\int dt'\,\xi_i^*(t)A_{ij}(t,t')\xi_j(t')$. The coupling $A_{ij}(t,t')$ between spin rotations at different times and different sites $i \neq j$ becomes

$$A_{ij}(t,t') = \frac{1}{4}\Big[R_{ij}^\downarrow(t,t')R_{ji}^\uparrow(t',t) + S_{ij}^\downarrow(t,t')S_{ji}^\uparrow(t',t)$$
$$-T_{ij}^\downarrow(t,t')G_{ji}^\uparrow(t',t) - G_{ij}^\downarrow(t',t)T_{ji}^\uparrow(t',t)\Big], \tag{7}$$

where $T_{ij}^\sigma(t,t') = \Sigma_{ij}^\sigma(t,t') + [\Sigma \star G \star \Sigma]_{ij}^\sigma(t,t')$, $R_{ij}^\sigma(t,t') = [G \star \Sigma]_{ij}^\sigma(t,t')$, $S_{ij}^\sigma(t,t') = [\Sigma \star G]_{ij}^\sigma(t,t')$, and $\star$ denotes the convolution. In general, these expressions include retardation

(memory) effects, as expressed by couplings $A_{ij}(t, t')$ depending on two time variables. This can be mapped onto an instantaneous exchange coupling when the rotations of the spin quantization axes are much slower than the electron dynamics, and, in particular, slower than time-dependent fluctuations of the local magnetic moments themselves. Averaging over the fast dynamics than gives

$$\overline{A_{ij}}(t) = \mathrm{Im} \int_0^\infty \mathrm{d}s \, A_{ij}^{\mathrm{ret}}(t, t - s). \tag{8}$$

Still, $\overline{A_{ij}}(t)$ contains not only the exchange interactions, but also the time-averaged reduction of the local spin by fluctuations. In the absence of symmetry breaking, the bare exchange interactions can be defined as

$$J_{ij}(t) = \frac{\overline{A_{ij}}(t)}{\langle \mathbf{S}_i(t) \cdot \mathbf{S}_j(t) \rangle}, \tag{9}$$

where $\langle \mathbf{S}_i(t) \cdot \mathbf{S}_j(t) \rangle$ is the equal-time spin correlation function. To evaluate these formulas, one has to compute the Greens functions and self-energies. A practical advantage of the general formulas is that they enable evaluation of exchange interactions in the collinear state, for which evaluation of the electronic dynamics is generally simpler. The implementation of equation (7)–(9) based on exact diagonalization is discussed in [21], while the implementation within nonequilibrium DMFT is detailed in [39], where $\langle \mathbf{S}_i(t) \cdot \mathbf{S}_j(t) \rangle$ in equation (9) is replaced by $\langle S_{iz}(t) \rangle \langle S_{jz}(t) \rangle$.

2.4. Floquet theory of nonequilibrium exchange

The above two methods for evaluation of nonequilbrium exchange interactions are in principle applicable to arbitrary electric fields. However, they do not give much analytical insight in how strong the exchange interactions can be modified. Considerable insight into this problem can be obtained by considering electric fields adjusted such that the electronic distribution is hardly changed. In this case, it becomes possible to generalize the perturbative result $J_{\mathrm{ex}} = 2t_0^2/U$, as was first demonstrated in [39] for time-periodic fields with frequencies non-resonant to direct electronic excitations. Considering a simple two-site Hubbard model, the equilibrium exchange interaction can be directly inferred form the singlet-triplet splitting: $J_{\mathrm{ex}} = (E_T - E_S)/2$, as illustrated in figure 3(a) for the $S_z = 0$ sector of the two-site Hubbard model at half-filling. Under time-periodic electric fields, one can apply Floquet's theorem [59, 60]. Solutions of the time-dependent Schrödinger equation are given in the form $|\psi(t)\rangle = \mathrm{e}^{-i\epsilon_\alpha t}|\psi_\alpha(t)\rangle$ where $|\psi_\alpha(t + T)\rangle = |\psi_\alpha(t)\rangle$ is time-periodic with a period $T = 2\pi/\omega$, and ϵ_α is a quasi-energy defined up to multiples of ω. A small part of the extended Floquet spectrum of the two-site system is illustrated in figure 3(b). In addition to the virtual hoppings that determine the equilibrium J_{ex} (blue arrows), there is virtual absorption and emission of photons to different Floquet sectors (red arrows). The mixing between these Floquet sectors results in a renormalization of the quasi-energy levels. The effective exchange interaction that emerges in the presence of the time-periodic field can then be extracted from the amplitude

dependent singlet-triplet splitting $\epsilon_T - \epsilon_S$ (figure 3(c)). For the single-band Hubbard model, the amplitude E_0 of the external field enters in calculations as the dimensionless driving strength $\mathcal{E} = eaE_0/\hbar\omega$, where e and a are unit charge and lattice spacing, respectively. For weak driving $\mathcal{E} \ll 1$, one obtains $J_{\mathrm{ex}} = 2t_0^2/U + \Delta J_{\mathrm{ex}}$ [39] with

$$\Delta J_{\mathrm{ex}} = \frac{\mathcal{E}^2 t_0^2}{2}\left(\frac{1}{U + \hbar\omega} + \frac{1}{U - \hbar\omega} - \frac{2}{U}\right). \tag{10}$$

Hence, depending on wether the frequency $\hbar\omega$ is below (above) the gap energy U, the net effect is an enhancement (reduction) of J_{ex}. For stronger driving strength we have $J_{\mathrm{ex}}(\mathcal{E}, \omega) = \sum_{m=-\infty}^\infty \frac{2t_0^2 J_{|m|}(\mathcal{E})^2}{U + m\hbar\omega}$ Interestingly, when $\mathcal{E}$ is of order one the terms with $U - m\hbar\omega$ can become strongly enhanced, leading to a sign reversal of J_{ex}. While originally derived on the basis of the two-site model, these results were soon confirmed based on more rigorous time-dependent canonical transformation techniques [61–63], illustrating that the essential physics is captured already within this simple model.

In addition, very similar results can be obtained for a three-site model, which takes into account explicitly that the hopping proceeds via an intermediate uncorrelated orbital and can be regarded as minimal model for superexchange [21]

$$\Delta J_{ex} = \frac{\mathcal{E}^2 t_0^4}{2}\left\{ \sum_\pm \left[\frac{1}{U_1 \pm \hbar\omega} + \frac{1}{U_1} \right]^2 \frac{1}{U \pm \hbar\omega} - \frac{4}{U_1^2 U} - \frac{4}{U_1^3} \right\}. \tag{11}$$

Here $U_1 = U + \Delta$, with Δ the energy splitting of the uncorrelated orbital with respect to the magnetic sites. The perturbative expressions equations (10) and (11) bear a close analogy with the derivation of the two-magnon Raman scattering Hamiltonian [64, 65] from the Hubbard model [66–68], see also section 4.3. The validity and usefulness of the Floquet picture are discussed in section 3.2 by direct comparison with the evaluation of the more general formulas introduced above.

3. Ultrafast control of J_{ex}

In principle, laser excitation can affect J_{ex} directly by modulating the electronic structure (electron hopping, Coulomb repulsion) and by creating a nonequilibrium distribution of photoexcited carriers (photodoping). In the latter case, this allows us to address the fundamental question how much time it takes before a static J_{ex} emerges from the full electronic dynamics and how much this J_{ex} is modified as compared to the equilibrium situation. Alternatively, the goal of modulating the electronic structure, is to achieve a control of J_{ex} which is reversible on ultrafast timescales, i.e. to give a controlled perturbation to J_{ex} during the application of the laser pulse, but leave the electronic state unexcited after the pulse is switched off. Both types of controlling J_{ex} are discussed below.

3.1. Photo-excitation

First we discuss the case of creating a nonequilbrium electronic distribution (photodoping), which was simulated for
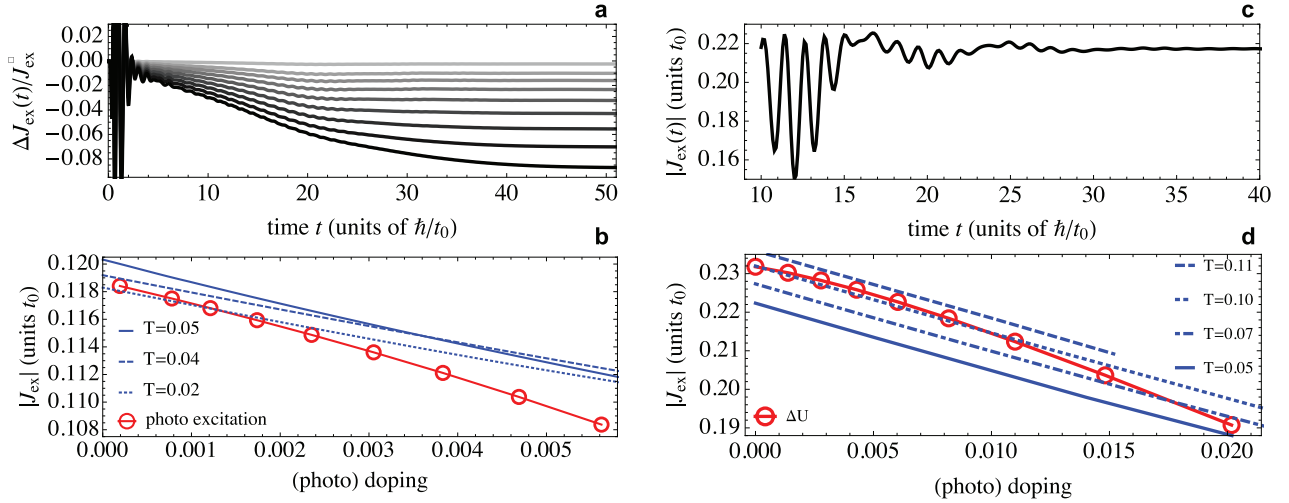
Figure 4. Ultrafast control of J_{ex} by photo doping in a Mott insulator. (a) time evolution of $\Delta J_{ex}(t)$ caused by excitation with an electric field pulse with strengths increasing from $|eaE_0/t_0| = 1 \ldots 5.5$ (hypercubic lattice in canted geometry, $U/t_0 = 8$). (b) comparison of the quasistationary nonequilibrium exchange interaction (red open circles) obtained from (a), with the equilibrium exchange interaction in the chemically doped system (blue lines). (c) time-dependent J_{ex} evaluated from the general formulas for a quench $U/t_0 = 4 \rightarrow 8$. (d) comparison as in (b) obtained using the general formulas for different interaction quenches ΔU. Both (c) and (d) are obtained on the Bethe lattice, with $U/t_0 = 8$ for the equilibrium results at chemical doping. Photo doping is here defined as the induced change $\Delta n = d + h - d_0 - h_0 = 2(d - d_0)$ of the doublon and hole densities d and h with respect to their equilibrium values d_0 and h_0. Reproduced with permission from [38], Copyright (2014) by The American Physical Society.

the AFM Mott insulator using nonequilibrium DMFT [38]. Results were obtained by evaluating the nonequilibrium J_{ex} in the canted geometry (section 2.2) as well as by evaluating the general nonequilibrium exchange formulas (section 2.3). For the canted geometry, the DMFT equations were solved on the hypercubic lattice and the dynamics was evaluated in response to a single-cycle pulse with center frequency $\hbar\omega = U$. The evolution of $\Delta J_{ex}(t)$ is shown in figure 4(a), which demonstrates that a stationary modified J_{ex} emerges already within a few tens of electron hopping times. A very similar time scale is found based on the general exchange formula (equation (9)), as shown in figure 4(c) (solid line). In this case, the DMFT equations were solved in a collinear setup on the Bethe lattice and a sudden change (quench) of the Coulomb interaction U was used to create a non-equilibrium electron distribution. Furthermore, it is found that the efficiency of modifying J_{ex} is determined by the number of photo-excited carriers, comparable to that of chemical doping. This is shown in the bottom panels, figures 4(b) and (d), by plotting the extracted exchange interaction in the quasistationary state as a function of the photodoping, together with equilibrium calculations with chemical doping with the same total number of carriers.

3.2. Modulating the electronic structure

Second we discuss the control of J_{ex} by modulating the electronic structure. In principle, the Floquet picture gives the effective exchange interaction under strictly periodic fields. However, in the long time limit isolated many-body systems can become infinitely excited and an effective low-energy description of the system is of limited use [69, 70]. Moreover, for short pulses with only a few number of cycles, it is *a priori* not clear how accurate the Floquet picture is. Below we review

simulation results, obtained with both exact diagonalization and nonequilibrium DMFT, which nevertheless confirm the Floquet picture, at least for the short-time dynamics on the time-scale defined by $\hbar/J_{ex}$.

A direct confirmation of equation (11) was obtained by evaluating equation (9) on a three-site cluster driven by a time-periodic field with an amplitude that is slowly ramped on, within about 10 cycles, while the electron dynamics is solved using exact diagonalization [21]. The effective exchange interaction was extracted by averaging over the period of the field:

$$J_{ij}^{\mathcal{E}}(t) = \frac{1}{T} \int_t^{t+T} ds\, J_{ij}(s), \qquad (12)$$

and found to be quasi-stationary for times sufficiently long after the ramp. Excellent quantitative agreement was obtained for the ratio $\Delta J/J \propto \mathcal{E}^2$ in the regime $\mathcal{E} \ll 1$. This is the regime that is most relevant to experiments on condensed matter systems and it was estimated that for model parameters typical for experiments on iron oxides a relative change $\Delta J/J \sim 1\%$ is achieved.

In a similar way, the period-averaged J_{ex} was compared in the canted DMFT setup [39]. In this case, a Gaussian envelope function was used containing about 15 cycles. For driving frequencies sufficiently far away from resonance, it is found that $\Delta J_{ex} \approx 0$ after the pulse (see figure 5(a), where $\hbar\omega = 3$ and $U = 10$), demonstrating that the electronic state of the system remains unexcited after the pulse has left and hence the exchange interaction can be controlled reversibly on ultrafast time scales. Furthermore, in accordance with the Floquet prediction, in the perturbative regime an enhancement (reduction) of J_{ex} is obtained for driving below (above) gap. This is shown in figure 5(b), by a quantitative comparison with the Floquet theory for the 'driving susceptibility' $\Delta J_{ex}/\left(J_{ex}\mathcal{E}^2\right)$.
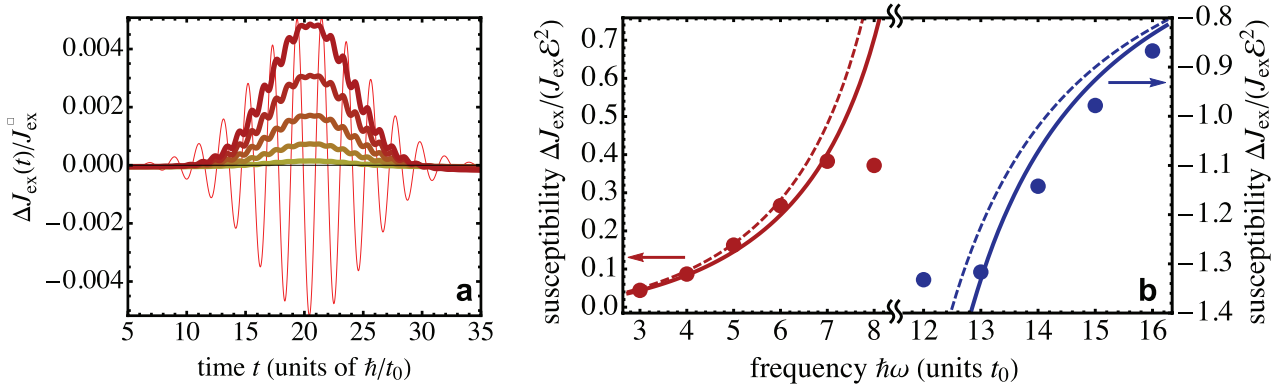
Figure 5. Control of J_{ex} by periodic driving. (a) Time-dependent change of the period-averaged exchange interaction (ΔJ_{ex}, thick lines) during the action of an oscillatory electric field pulse (thin lines), with driving frequency $\hbar\omega = 3$ below the Mott gap. Different colours correspond to results obtained with different amplitude E_0 of the electric field, increasing from light to dark. Numerical results were obtained using Dynamical Mean Field Theory (DMFT) for the hyper-cubic lattice at $U = 10$ and initial temperature $T = 0.025$. (b) The driving susceptibility $\Delta J_{ex}/(J_{ex}\mathcal{E}^2)$ for $\mathcal{E} \to 0$ for frequencies above (blue, right vertical axis) and below gap (red, left vertical axis), obtained from DMFT for the hyper-cubic lattice (disks), from the numerical Floquet spectrum of a two-site Hubbard cluster (solid lines), and from the perturbative result equation (10) (dashed lines). Reproduced with permission from [39].

The solid symbols are obtained from running several DMFT calculations at increasing field strength (different colors in figure 5(a)), while the dashed and solid lines are based on the perturbative result (equation (10) and the full Floquet spectrum (non-perturbative in t_0/U) by evaluating the derivative $dJ_{ex}/d\mathcal{E}^2$ at $\mathcal{E} \to 0$, respectively. Away from the band edge, where the system is photo-excited (section 3.1), the frequency dependence matches very well, being even in quantitative agreement for the lowest frequencies below gap. Hence, the Floquet theory forms a useful guide for understanding the ultrafast and reversible control of J_{ex} in condensed matter systems by photo-assisted hopping.

4. Manipulation of magnetism

Modelling how magnetic order can be manipulated by short time-dependent perturbations of exchange interactions can be addressed on several levels, four of which are discussed here. First, we focus on macrospin theory, which is suitable to describe homogenous spin precession and was used to establish the link between the experimentally observed AFM resonances and the sub-picosecond control of exchange interactions [21]. Second, atomistic spin dynamics simulations are used to investigate the response of the spin temperature to sudden changes in J_{ex} [40]. Third, harmonic magnon theory is used to model impulsively stimulated two-magnon Raman scattering due to perturbations of J_{ex}, leading to longitudinal macrospin dynamics [22, 71, 72]. Finally, the quantum spin dynamics of a one-dimensional chain is studied, leading to effective time reversal under influence of a change of sign of J_{ex} by periodically modulating the electronic structure [39].

4.1. Excitation of spin precession

Modeling of macroscopic spin precession can be conveniently done by solving the multi-scale problem on the basis of the macrospin approximation. In this case, each of the magnetic sublattices is treated as an effective macrospin with dynamics

governed by the Landau-Lifshitz equation. As introduced in section 2.2, we can also use the Landau-Lifshitz equation to infer an effective $J_{ex}(t)$ from an observed spin precession. Here, we focus how this approach was used to provide experimental evidence for an ultrafast control of exchange interactions.

Instead of a canting induced by an external magnetic field, the experiments were performed on iron oxides that are intrinsically canted due to an additional antisymmetric, so-called Dzyaloshinskii–Moriya interaction and described by $H_{DM} = \mathbf{D} \cdot \sum_{ij} (\mathbf{S}_i \times \mathbf{S}_j)$. General symmetry arguments can be used to prove that perturbations to both J_{ex} and $\mathbf{D}$ contain an intensity dependent contribution ($\propto|\mathbf{E}|^2$). For example, by using equation (10) and assuming a simple cubic lattice, this also follows directly from the microscopic model. In the macrospin approximation, the torque on $\langle\mathbf{S}_1\rangle$ due to $\langle\mathbf{S}_2\rangle$ is given by $\mathbf{T}_1 = -\langle\mathbf{S}_1\rangle \times \Delta\mathbf{B}_{ex}$, where

$$\Delta\mathbf{B}_{ex} = \sum_j \Delta J_{1j}\langle\mathbf{S}_2\rangle = \left(2\alpha E_x^2 + 2\alpha E_y^2 + 2\alpha E_z^2\right)\langle\mathbf{S}_2\rangle = 2\alpha|\mathbf{E}|^2\langle\mathbf{S}_2\rangle,$$

(13)

where the summation is over the six nearest neighbor bonds. Defining $\mathbf{E} = E_0\mathbf{e}$, $\mathbf{e}$ the unit vector of polarization, we recover $\alpha|\mathbf{E}|^2 = \Delta J_{ex}$, with ΔJ_{ex} defined by equation (10). Hence, although only those exchange bonds are perturbed that have a projection along the electric field, it follows that the torque, which is a sum over all bonds, is independent on the polarization of light. This isotropy is in strong contrast with previously reported mechanisms for the optical excitation of spin resonances, such as the inverse Faraday [3] and inverse Cotton–Motton effect [73], which depend on the helicity of light and on the orientation of the polarization with respect to the magnetization, respectively. Hence, the key experimental signature of optical perturbation of exchange interactions, is an isotropic, polarization independent excitation of the spin resonance. This is exactly what has been observed in the experiments on femtosecond laser excitation of iron oxides, where the subsequent spin dynamics was detected using THz emission spectroscopy [21]. A quantitative analysis supports

the sub-picosecond time scale at which ΔJ_{ex} can occur, consistent with the theoretical results discussed in section 3. Moreover, in the same and similar materials not only the control of J_{ex} between transition metal ions was found, but also the first indications were reported for the control of J_{ex} between the rare-earth ions [74, 75]. We emphasize, however, that the experiment [21] is sensitive to an ultrafast perturbation of the *ratio* $|\mathbf{D}|/J_{ex}$ and hence does not provide a direct proof of the modification of J_{ex} alone.

4.2. Cooling by perturbation of exchange

Perturbation of exchange interactions can also influence the relaxation and internal equilibration of the spin degrees of freedom. To simulate such effects, the dynamics of an ensemble of spins has be be solved. In the regime where a classical description is valid, this can be done conveniently on the basis of atomistic spin dynamics (ASD) [76, 77]. Within ASD, the dynamics of each atomic spin in the system evolves according to the stochastic Landau-Lifshitz equation

$$\hbar \frac{d\mathbf{S}_i}{dt} = -\mathbf{S}_i \times \left(\mathbf{B}_i + \mathbf{B}_i^{fl}(t)\right) - \frac{\alpha}{S_i}\mathbf{S}_i \times \left[\mathbf{S}_i \times \left(\mathbf{B}_i + \mathbf{B}_i^{fl}(t)\right)\right]$$

(14)

which describe the motion of the classical spins $\mathbf{S}_i$ in an effective magnetic field $\mathbf{B}_i$, calculated from $\mathbf{B}_i = -\partial H_{spin}/\partial \mathbf{S}_i$. $\mathbf{B}_i^{fl}(t)$ is a stochastic magnetic field with a Gaussian distribution. By the fluctuation-dissipation theorem, the magnitude of $\mathbf{B}_i^{fl}(t)$ is related to the dimensionless damping parameter α. ASD simulations in response to perturbations of exchange interactions were carried out for CuO [40] based on equilibrium exchange parameters computed from first principles, which involves both bilinear Heisenberg exchange and biquadratic exchange interactions [78]. Figure 6 shows the evolution of the temperature of the system as evaluated by fitting a Boltzmann distribution to the energy distribution of the spins, after introducing vacancies (sites without spin) with a concentration $x = 0.02$. Interestingly, starting in the low-temperature collinear antiferromagnetic phase, the system evolves within the AFM phase by rapid internal equilibration which reduces the temperature. This can be explained as an ultrafast magneto-caloric effect, where the closed system follows a constant entropy curve in response to lowering the strength of the exchange fields. This interpretation was confirmed by comparison with the equilibrium entropy per spin at different concentrations x, showing close to quantitative agreement. When the system is coupled to a heat bath, still a transient drop is observed, after which the system relaxes to the temperature of the heat bath (dashed line in figure 6). For small x, qualitatively similar results were obtained by a step-like reduction of exchange parameters. Although several aspects of existing experimental work [79] on laser-induced dynamics in CuO are not captured by the simulations shown here (see [40] for a detailed discussion), the results do suggest new opportunities to achieve ultrafast laser-induced cooling of magnets by optical perturbations of exchange, strongly contrasting the laser-induced heating commonly observed in metallic magnets [6].
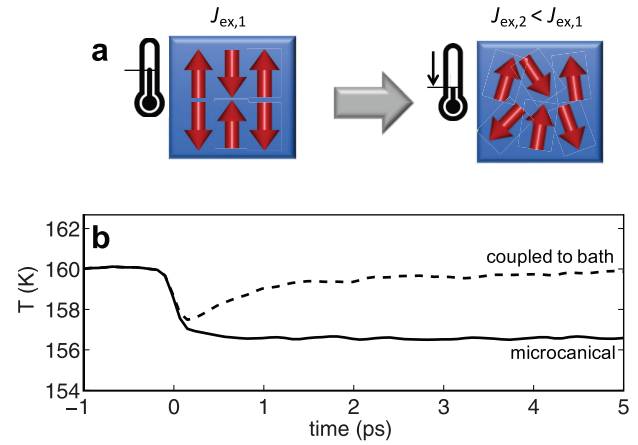

Figure 6. Rapid cooling by perturbations of exchange interactions. (a) Illustration of cooling by reduction of J_{ex}. (b) results of atomistic spin dynamics simulations where the response of the spin temperature is measured after a step-like change of exchange interactions, as modelled by the introduction of a fraction of $x = 0.02$ vacancies at $t = 0$ ps. Solid lines show the microcanonical evolution, dashed lines include coupling to the bath, with a dimensionless coupling strength $\alpha = 0.01$. Reproduced with permission from [40]. Copyright (2016) by The American Physical Society.

4.3. Excitation of coherent longitudinal spin dynamics

In collinear antiferromagnets, perturbations of exchange interactions do not give rise to excitation of the homogenous antiferromangetic resonance (AFMR) mode, since the effective field generated by the perturbation of J_{ex} is collinear with the sublattice magnetization and therefore the torque vanishes: $\mathbf{T}_1 = -\langle\mathbf{S}_1\rangle \times 2\Delta J_{ex}\langle\mathbf{S}_2\rangle = 0$. Nevertheless, it was recently reported that coherent *longitudinal* oscillations of the AFM order parameter can be triggered by ultrashort perturbations of exchange interactions [22]. Modeling of such longitudinal dynamics goes beyond the macrospin approximation employed in section 4.1, which conserves the length of the sublattice magnetization $|\langle\mathbf{S}_i\rangle|$. Extending on previous results [71, 72], it was found that the longitudinal dynamics emerges naturally within harmonic magnon theory [22] due to the impulsive excitation of pairs of magnons with opposite $\mathbf{k}$ by perturbations of J_{ex}. Here we discuss these theoretical results by showing that they can be understood from a simple quantum-mechanical two-level system.

Following [22, 71], we start from an unperturbed Heisenberg Hamiltonian $H_0 = J_{ex}\sum_{i\delta}\mathbf{S}_i\mathbf{S}_{i+\delta}$. Perturbations to J_{ex} depend on the orientation of the electric field and for the simple cubic lattice it follows from equation (10) that we can write $\delta H = \Delta J_{ex}\sum_{i\delta}(\mathbf{e}\cdot\boldsymbol{\delta})^2\mathbf{S}_i\mathbf{S}_{i+\delta}$. Here $\boldsymbol{\delta}$ is the unit vector connecting two adjacent sites on different sublattices and $\mathbf{e}$ is the unit vector of the polarization of light. More generally, one can use here also the phenomenological second order Raman tensor and the present description is analogous to the one used for impulsive Raman scattering of phonons [80]. Magnons are described in the usual way by introducing Holstein–Primakov bosons $a_\mathbf{k}, b_\mathbf{k}$ for spins in different sublattices [81, 82]. Keeping only the terms bilinear in the magnon operators we have

$$H_0' = zJ_{\mathrm{ex}}S \sum_{\mathbf{k}} \left[\gamma_{\mathbf{k}} \left(a_{\mathbf{k}} b_{-\mathbf{k}} + a_{\mathbf{k}}^{\dagger} b_{-\mathbf{k}}^{\dagger} \right) + \left(a_{\mathbf{k}}^{\dagger} a_{\mathbf{k}} + b_{-\mathbf{k}}^{\dagger} b_{-\mathbf{k}} \right) \right], \tag{15}$$

$$\delta H' = z\Delta J_{\mathrm{ex}}S \sum_{\mathbf{k}} \left[\xi_{\mathbf{k}} \left(a_{\mathbf{k}} b_{-\mathbf{k}} + a_{\mathbf{k}}^{\dagger} b_{-\mathbf{k}}^{\dagger} \right) + \left(a_{\mathbf{k}}^{\dagger} a_{\mathbf{k}} + b_{-\mathbf{k}}^{\dagger} b_{-\mathbf{k}} \right) \right]. \tag{16}$$

Here $\gamma_{\mathbf{k}} = \frac{1}{z} \sum_{\boldsymbol{\delta}} \exp(i\mathbf{k} \cdot \boldsymbol{\delta})$ and $\xi_{\mathbf{k}} = \frac{1}{z} \sum_{\boldsymbol{\delta}} (\mathbf{e} \cdot \boldsymbol{\delta})^2 \exp(i\mathbf{k} \cdot \boldsymbol{\delta})$. Due to the exchange interaction between spins of different sublattices, H_0 is not diagonal in the magnon operators $a_{\mathbf{k}}, b_{\mathbf{k}}$. To diagonalize H_0, composite magnons are introduced by a Bogoliubov transform

$$a_{\mathbf{k}} = u_{\mathbf{k}} \alpha_{\mathbf{k}} + v_{\mathbf{k}} \beta_{-\mathbf{k}}^{\dagger}, \tag{17}$$

$$b_{\mathbf{k}} = u_{\mathbf{k}} \beta_{\mathbf{k}} + v_{\mathbf{k}} \alpha_{-\mathbf{k}}^{\dagger}. \tag{18}$$

where the coefficients $u_{\mathbf{k}}, v_{\mathbf{k}}$ are chosen such that the off-diagonal terms vanish, yielding $H_0' = \sum_{\mathbf{k}} \hbar\omega_{\mathbf{k}} \left(\alpha_{\mathbf{k}}^{\dagger} \alpha_{\mathbf{k}} + \beta_{\mathbf{k}}^{\dagger} \beta_{\mathbf{k}} \right)$, where $\hbar\omega_{\mathbf{k}} = zJ_{\mathrm{ex}}S\sqrt{1 - \gamma_{\mathbf{k}}^2}$. However, the same transformation does not diagonalize $\delta H'$:

$$\delta H' = \sum_{\mathbf{k}} \delta\hbar\omega_{\mathbf{k}} \left(\alpha_{\mathbf{k}}^{\dagger} \alpha_{\mathbf{k}} + \beta_{\mathbf{k}}^{\dagger} \beta_{\mathbf{k}} \right) + V_{\mathbf{k}} \left(\alpha_{\mathbf{k}} \beta_{-\mathbf{k}} + \alpha_{\mathbf{k}}^{\dagger} \beta_{-\mathbf{k}}^{\dagger} \right), \tag{19}$$

where $\delta\hbar\omega_{\mathbf{k}} = z\Delta J_{\mathrm{ex}}S \left(1 - \xi_{\mathbf{k}}\gamma_{\mathbf{k}}\right)/\sqrt{1 - \gamma_{\mathbf{k}}^2}$, $V_{\mathbf{k}} = z\Delta J_{\mathrm{ex}}S$ $(\xi_{\mathbf{k}} - \gamma_{\mathbf{k}})/\sqrt{1 - \gamma_{\mathbf{k}}^2}$. Since in general $\xi_{\mathbf{k}} \neq \gamma_{\mathbf{k}}$, pairs of magnons with opposite $\mathbf{k}$ are excited due to the second term in equation (19). From the structure of this term, we see that the response to time-dependent perturbations $\Delta J_{\mathrm{ex}}(t)$ maps onto the solution of a collection of independent two-level systems for each pair $\mathbf{k}, -\mathbf{k}$. In particular, starting from the ground state $|g_{\mathbf{k}}\rangle = |0\rangle|0\rangle$, $\delta H'$ only induces couplings to excited states $|e_{\mathbf{k}}\rangle = \alpha_{\mathbf{k}}^{\dagger} \beta_{-\mathbf{k}}^{\dagger} |0\rangle|0\rangle$ and we have a two-level system specified by

$$\langle g_{\mathbf{k}}|H_0' + \delta H'|g_{\mathbf{k}}\rangle = 0 \tag{20}$$

$$\langle e_{\mathbf{k}}|H_0' + \delta H'|e_{\mathbf{k}}\rangle = 2\left[\hbar\omega_{\mathbf{k}} + \delta\hbar\omega_{\mathbf{k}}(t)\right] \tag{21}$$

$$\langle g_{\mathbf{k}}|H_0' + \delta H'|e_{\mathbf{k}}\rangle = \langle e_{\mathbf{k}}|H_0' + \delta H'|g_{\mathbf{k}}\rangle^* = V_{\mathbf{k}}(t). \tag{22}$$

The solution can be obtained by writing $|\psi_{\mathbf{k}}(t)\rangle = c_{\mathbf{k}}(t)|g_{\mathbf{k}}\rangle + d_{\mathbf{k}}(t)|e_{\mathbf{k}}\rangle$. For impulsive excitation we write $V_{\mathbf{k}}(t) = \tau\hbar\overline{V_{\mathbf{k}}}\delta(t)$ and obtain analytical expressions valid for $t \gg \tau$:

$$c_{\mathbf{k}}(t) = c_{\mathbf{k}}(0)\cos(\tau\overline{V_{\mathbf{k}}}), \quad d_{\mathbf{k}}(t) = -ic_{\mathbf{k}}(0)\sin(\tau\overline{V_{\mathbf{k}}})e^{i2\omega_{\mathbf{k}}t}, \tag{23}$$

where we for simplicity neglected a small phase accumulated due to $\delta\hbar\omega_{\mathbf{k}}(t)$. Longitudinal dynamics follows by evaluating

$$\langle L_z(t)\rangle = \sum_k \langle\psi_{\mathbf{k}}(t)|\hat{L}_z|\psi_{\mathbf{k}}(t)\rangle = NS - \frac{2}{N}\sum_{\mathbf{k}} \langle\psi_{\mathbf{k}}(t)|a_{\mathbf{k}}^{\dagger}a_{\mathbf{k}} + b_{\mathbf{k}}^{\dagger}b_{\mathbf{k}}|\psi_{\mathbf{k}}(t)\rangle, \tag{24}$$

where N is the total number of spins and $\hat{L}_z = \sum_{i,j} (S_{iz} - S_{jz})$ is the z-component of the antiferromagnetic vector $\mathbf{L}$. Substituting the Bogoliubov transformation and keeping only terms linear in $\overline{V_{\mathbf{k}}}$ ($\Delta J_{\mathrm{ex}} \ll J_{\mathrm{ex}}$), we find that the dynamics of

$\langle L_z(t)\rangle$ is determined by the terms $\langle\psi_{\mathbf{k}}(t)|\alpha_{\mathbf{k}}\beta_{-\mathbf{k}} + \alpha_{\mathbf{k}}^{\dagger}\beta_{-\mathbf{k}}^{\dagger}$ $|\psi_{\mathbf{k}}(t)\rangle = c_{\mathbf{k}}^*(0)d_{\mathbf{k}}(t) + c_{\mathbf{k}}(0)d_{\mathbf{k}}^*(t) = -2c_{\mathbf{k}}^2(0)\overline{V_{\mathbf{k}}}\sin(2\omega_{\mathbf{k}}t)$, finally giving

$$\langle L_z(t)\rangle = \mathrm{const} - 2\sum_{\mathbf{k}} \frac{\tau\overline{V_{\mathbf{k}}}c_{\mathbf{k}}^2(0)\gamma_{\mathbf{k}}}{\sqrt{1 - \gamma_{\mathbf{k}}^2}}\sin(2\omega_{\mathbf{k}}t). \tag{25}$$

Although qualitatively the dynamics of the longitudinal dynamics described by this equation is very different from homogenous spin precession, the solution of the problem has a very similar mathematical structure. In particular, due to the mapping onto a collection of independent two-level systems of composite magnons, the solution of the time-dependent wave function can be represented on the Bloch sphere, analogous to the case of homogenous spin precession described by a two-level system [83, 84]. This is illustrated in figure 7, where the north and south pole represent the ground and two-magnon excited state, respectively. During the application of the optical pulse, perturbations of exchange interactions bring the system into a super position of the ground and excited state, as indicated by the red line. After the pulse is gone, this coherence $c_{\mathbf{k}}^*(0)d_{\mathbf{k}}(t) + c_{\mathbf{k}}(0)d_{\mathbf{k}}^*(t)$ remains and the wave function (blue arrow) follows the blue trajectory on the Bloch sphere. For the two-magnon case, the excited state comprises two magnons and hence the oscillation occurs at twice the single magnon frequency.

In principle magnons of all $\mathbf{k}$ contribute to the dynamics of L_z. However, close to the Brillouin zone-boundary the magnon density of states peaks due to the vicinity of a van-Hove singularity. Therefore, magnons close to the zone edge ($\gamma_{\mathbf{k}}^2 \ll 1$) give the dominant contribution and L_z oscillates at $2\omega_{\mathbf{k}} = 2zJ_{\mathrm{ex}}S\sqrt{1 - \gamma_{\mathbf{k}}^2}/\hbar \approx 2zJ_{\mathrm{ex}}S/\hbar$. This gives coherent spin dynamics in the femtosecond regime [22], which is much faster than the frequency of AFM resonance ($\omega \sim S\sqrt{J_{\mathrm{ex}}K}/\hbar$, where $K \ll J_{\mathrm{ex}}$ the anisotropy energy). While we limited ourselves here to a simple two-level description of existing theoretical results, it will be very interesting to better understand this regime of longitudinal spin dynamics and in particular the relation with quantum effects such as the magnon squeezing discussed in earlier works [71, 72].

4.4. Effective time reversal

For sufficiently strong driving strength, the Floquet theory predicts that even the sign of the exchange interaction can be changed. A naive equilibrium analysis would suggest the system evolves into a ferromagnetic state. However, in dynamics this is not possible, since the total spin is conserved under time evolution with the Heisenberg Hamiltonian. Nevertheless, even if the system remains AFM, a change of sign of J_{ex} allows for a very non-trivial way to control the spin dynamics, namely, to reverse the time evolution of the undriven system. Here we show the example of the one-dimensional spin chain [39]. Opposed to the examples discussed before, for small systems the full electronic dynamics of the Hubbard model, including their spin degrees of freedom, is computationally tractable with exact diagonalization. The results of such simulations
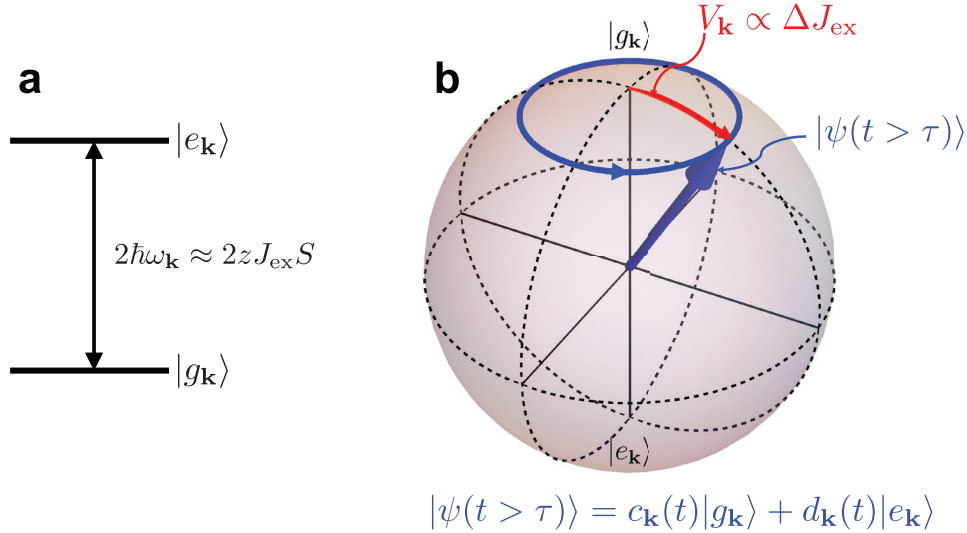
$$|\psi(t > \tau)\rangle = c_{\mathbf{k}}(t)|g_{\mathbf{k}}\rangle + d_{\mathbf{k}}(t)|e_{\mathbf{k}}\rangle$$

Figure 7. (a) Two-level system with approximate splitting $2\hbar\omega_{\mathbf{k}} \propto 2J_{\mathrm{ex}}$. (b) Bloch sphere representation of the two-level system with north and south pole representing the ground and two-magnon excited state, respectively. The red line indicates the effect of the perturbation $V_{\mathbf{k}} \propto \Delta J_{\mathrm{ex}}$ which brings the system in a super position of the ground sate and excited state (blue arrow), after which the wave function follows the blue trajectory, oscillating at twice the single magnon frequency. Note that for the two-magnon case, unlike for homogenous spin precession, the projections of $|\psi(t)\rangle$ onto the cartesian axes do not correspond to different components of the homogenous magnetization.

for a chain of $N = 10$ sites are shown in figure 8. To demonstrate the effective time-reversal, the system is prepared in the uncorrelated Néel state, which is a highly excited state of the one-dimensional chain and evolution under the unperturbed Hamiltonian will show a rapid decrease of the staggered magnetization $M = \frac{1}{N}\sum_{i=1}^{N}(-1)^{i+1}\langle \hat{n}_{i\uparrow} - \hat{n}_{i\downarrow}\rangle$. Subsequently, a time-periodic electric field is ramped on (figure 8(a)), with Floquet amplitude $\mathcal{E} = 3.4$ and frequency $\hbar\omega/U = 0.6$, for which the Floquet theory for a two-site model predicts a reversal of the exchange coupling. Under the periodic driving, one indeed observes a near perfect reversal of the dynamics of $M(t)$ in figure 8(b), which almost completely recovers the initial value $M(t = 0)$ around $t = 100$. Subsequently, $M(t)$ is reduced again by further evolution in the reverse direction. This continues until the field is ramped off, after which one observes that the free evolution brings the system again back to the initial state, from which the same rapid decay of $M(t)$ is observed as for the initial free evolution. This result can be well understood from the time-evolution of the pure quantum spin Hamiltonian. Propagation over a time interval t with the unperturbed Hamiltonian is given by the evolution operator $\mathcal{U}_{\mathrm{AFM}} = \exp(-iH_{\mathrm{ex}}t/\hbar)$. This evolution is exactly reversed by propagation with J'_{ex} of opposite sign over a time interval $t' = |J_{\mathrm{ex}}/J'_{\mathrm{ex}}|t$, since for the ferromagnetic (FM) time evolution we have $\mathcal{U}_{\mathrm{FM}} = \exp(-iH'_{\mathrm{ex}}t'/\hbar) = \exp(+iH_{\mathrm{ex}}t/\hbar) = \mathcal{U}_{\mathrm{AFM}}^{-1}$. Hence, the full dynamics of the Hubbard model very nicely resembles the dynamics expected from the pure spin model with dynamically perturbed J_{ex}, further confirming the reversibility of the optical control of J_{ex}. Interestingly, we observe that analogous to the dynamics discussed in section 4.3, the evolution shows coherent purely longitudinal spin dynamics on the time scale determined by J_{ex}. While the present results may not be directly relevant for condensed matter systems due to the strong field strengths required ($\mathcal{E} \sim 1$ corresponds
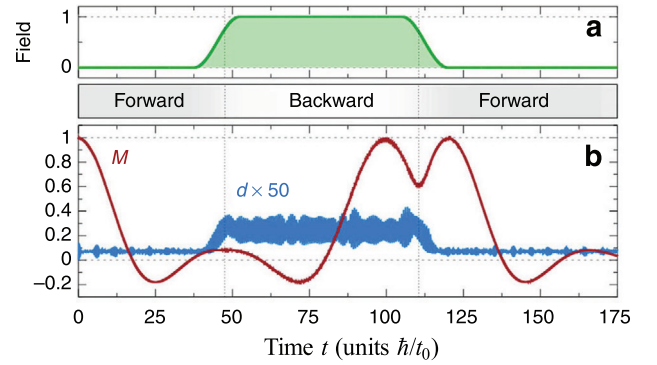

Figure 8. Effective time reversal of spin dynamics. (a) Field envelope with cosine-shaped ramps of length $\Delta t = 15$ around $t_1 = 45$ and $t_2 = 112.5$. The bar below the field envelope indicates forward (grey) and backward (white) time evolution when the field is off and on, respectively. (b) Time evolution of staggered magnetization M (red) and total double occupation d (blue), scaled by a factor of 50, of a 10-site Hubbard chain, showing free evolution for times to $t < 37.5$ and $t > 120$ and evolution under an additional periodic driving at frequency $\omega/U = 0.6$ and Floquet amplitude $\mathcal{E} = 3.4$ in between. Reproduced with permission from [39].

to fields $E_0 \sim 1$ V $\overset{\circ}{\mathrm{A}}^{-1}$), they provide novel possibilities to study the reversibility of quantum many body dynamics in cold atom systems.

5. Conclusion and outlook

The aim of this review was to describe the recent theoretical and computation work focused on the description of both the control of exchange interactions under electronic nonequilibrium conditions as well as the response of antiferromagnetic order to such perturbations. Interestingly, besides new ways

to excite spin precession, it was found that qualitatively new relaxation and coherent spin dynamics emerges due to ultrafast perturbations of exchange interactions in antiferromagnets. While the simulations on the control of the Heisenberg exchange interaction J_{ex} reviewed here are based on the prototype single-band Hubbard model, natural extensions are to study systems with competing interactions, which in general requires studying multi-band systems. Recently, competing exchange interactions have already been studied for effective single-band systems with different underlying lattice geometry and by including higher order terms in the hopping t_0 [85–87]. In addition, also the first studies on multi-orbital systems has been performed [88, 89]. Interestingly, beyond the control with laser pulses in the optical regime, [89, 90] also discuss the control by THz electric field fields and transients, which suggest new opportunities for non-linear spin responses to THz pulses [91–94], involving both the electric and the magnetic field of the THz pulse. For the manipulation of magnetic order, it will be very interesting to further study the influence of competing exchange interactions for the cooling by perturbations of exchange interactions. This potentially can lead to very efficient cooling strategies, since the exchange fields are much stronger than conventional external magnetic fields, suggesting high potential for magnetic refrigeration applications [95]. Finally, it will be very interesting to go beyond the limitations of the harmonic magnon theory and the exact diagonalization to characterize and further explore the regime of coherent longitudinal spin dynamics, which keeps great promise for finding new physical phenomena in the short-time dynamics of macroscopic magnetic order out of equilibrium.

Acknowledgment

References

[1] Beaurepaire E, Merle J-C, Daunois A and Bigot J-Y 1996 Ultrafast spin dynamics in ferromagnetic nickel *Phys. Rev. Lett.* **76** 4250–3

[2] van Kampen M, Jozsa C, Kohlhepp J T, LeClair P, Lagae L, de Jonge W J M and Koopmans B 2002 All-optical probe of coherent spin waves *Phys. Rev. Lett.* **88** 227201

[3] Kimel A, Kirilyuk A, Usachev P, Pisarev R V, Balbashov A M and Rasing T 2005 Ultrafast non-thermal control of magnetization by instantaneous photomagnetic pulses *Nature* **435** 655

[4] Stanciu C D, Hansteen F, Kimel A V, Kirilyuk A, Tsukamoto A, Itoh A and Rasing T 2007 All-optical magnetic recording with circularly polarized light *Phys. Rev. Lett.* **99** 047601

[5] Vahaplar K, Kalashnikova A M, Kimel A V, Hinzke D, Nowak U, Chantrell R, Tsukamoto A, Itoh A, Kirilyuk A and Rasing T 2009 Ultrafast path for optical magnetization reversal via a strongly nonequilibrium state *Phys. Rev. Lett.* **103** 117201

[6] Kirilyuk A, Kimel A V and Rasing T 2010 Ultrafast optical manipulation of magnetic order *Rev. Mod. Phys.* **82** 2731–84

[7] Ostler T *et al* 2012 Ultrafast heating as a sufficient stimulus for magnetization reversal in a ferrimagnet *Nat. Commun.* **3** 666

[8] Radu I *et al* 2011 Transient ferromagnetic-like state mediating ultrafast reversal of antiferromagnetically coupled spins *Nature* **472** 205

[9] Mathias S *et al* 2012 Probing the timescale of the exchange interaction in a ferromagnetic alloy *Proc. Natl Acad. Sci.* **109** 4792–7

[10] Radu I *et al* 2015 Ultrafast and distinct spin dynamics in magnetic alloys *Spin* **05** 1550004

[11] Lambert C-H *et al* 2014 All-optical control of ferromagnetic thin films and nanostructures *Science* **345** 1337–40

[12] Stupakiewicz A, Szerenos K, Afanasiev D, Kirilyuk A and Kimel A V 2017 Ultrafast nonthermal photo-magnetic recording in a transparent medium *Nature* **542** 71–4

[13] Rhie H-S, Dürr H and Eberhardt W 2003 Femtosecond electron and spin dynamics in ni/w(1 1 0) films *Phys. Rev. Lett.* **90** 247201

[14] Carley R *et al* 2012 Femtosecond laser excitation drives ferromagnetic gadolinium out of magnetic equilibrium *Phys. Rev. Lett.* **109** 057401

[15] Frietsch B, Bowlan J, Carley R, Teichmann M, Wienholdt S, Hinzke D, Nowak U, Carva K, Oppeneer P M and Weinelt M 2015 Disparate ultrafast dynamics of itinerant and localized magnetic moments in gadolinium metal *Nat. Commun.* **6** 8262

[16] Eich S *et al* 2017 Band structure evolution during the ultrafast ferromagnetic-paramagnetic phase transition in cobalt *Sci. Adv.* **3** e1602094

[17] Melnikov A, Radu I, Bovensiepen U, Krupin O, Starke K, Matthias E and Wolf M 2003 Coherent optical phonons and parametrically coupled magnons induced by femtosecond laser excitation of the Gd(0 0 0 1) surface *Phys. Rev. Lett.* **91** 227403

[18] Ju G *et al* 2004 Ultrafast generation of ferromagnetic order via a laser-induced phase transformation in ferh thin films *Phys. Rev. Lett.* **93** 197403

[19] Thiele J, Buess M and Back C H 2004 Spin dynamics of the antiferromagnetic-to-ferromagnetic phase transition in ferh on a sub-picosecond time scale *Appl. Phys. Lett.* **85** 2857

[20] Subkhangulov R R, Henriques A B, Rappl P H O, Abramof E, Rasing T and Kimel A V 2014 All-optical manipulation and probing of the d*f* exchange interaction in eute *Sci. Rep.* **4** 4368

[21] Mikhaylovskiy R V *et al* 2015 Ultrafast optical modification of exchange interactions in iron oxides *Nat. Commun.* **6** 8190

[22] Bossini D, Dal Conte S, Hashimoto Y, Secchi A, Pisarev R, Rasing T, Cerullo G and Kimel A V 2016 Macrospin dynamics in antiferromagnets triggered by sub-20 femtosecond injection of nanomagnons *Nat. Commun.* **7** 10645

[23] Loss D and DiVincenzo Jan D P 1998 Quantum computation with quantum dots *Phys. Rev.* A **57** 120–6

[24] Shahbazyan T, Perakis I and Raikh M 2000 Spin correlations in nonlinear optical response: light-induced Kondo effect *Phys. Rev. Lett.* **84** 5896–9

[25] Piermarocchi C, Chen P, Sham L and Steel D 2002 Optical RKKY interaction between charged semiconductor quantum dots *Phys. Rev. Lett.* **89** 167402

[26] Duan L-M, Demler E and Lukin Aug M D 2003 Controlling spin exchange interactions of ultracold atoms in optical lattices *Phys. Rev. Lett.* **91** 090402

[27] Trotzky S, Cheinet P, Flling S, Feld M, Schnorrberger U, Rey A M, Polkovnikov A, Demler E A, Lukin M D and Bloch I 2008 Time-resolved observation and control of superexchange interactions with ultracold atoms in optical lattices *Science* **319** 295–9

[28] Chen Y-A, Nascimbene S, Aidelsburger M, Atala M, Trotzky S and Bloch I 2011 Controlling correlated tunneling and superexchange interactions with ac-driven optical lattices *Phys. Rev. Lett.* **107** 210405

[29] Wall S, Prabhakaran D, Boothroyd A T and Cavalleri Aug A 2009 Ultrafast coupling between light, coherent lattice vibrations, and the magnetic structure of semicovalent LaMnO$_3$ *Phys. Rev. Lett.* **103** 097402

[30] Först M *et al* 2011 Driving magnetic order in a manganite by ultrafast lattice excitation *Phys. Rev.* B **84** 241104

[31] Li T *et al* 2013 Femtosecond switching of magnetism via strongly correlated spin-charge quantum excitations *Nature* **496** 69–73

[32] Nagaev E L 1988 Photoinduced magnetism and conduction electrons in magnetic semiconductors *Phys. Status Solidi* b **145** 11–64

[33] Kane B 1998 A silicon-based nuclear spin quantum computer *Nature* **393** 133–7

[34] Piermarocchi C and Quinteiro G F 2004 Coherent optical control of spin–spin interaction in doped semiconductors *Phys. Rev.* B **70** 235210

[35] Fernández-Rossier J, Piermarocchi C, Chen P, MacDonald A and Sham L 2004 Coherently photoinduced ferromagnetism in diluted magnetic semiconductors *Phys. Rev. Lett.* **93** 127201

[36] Wang J, Cotoros I, Dani K, Liu X, Furdyna J and Chemla D 2007 Ultrafast enhancement of ferromagnetism via photoexcited holes in GaMnAs *Phys. Rev. Lett.* **98** 217401

[37] Matsubara M, Schroer A, Schmehl A, Melville A, Becher C, Trujillo-Martinez M, Schlom D G, Mannhart J, Kroha J and Fiebig M 2015 Ultrafast optical tuning of ferromagnetism via the carrier density *Nat. Commun.* **6** 6724

[38] Mentink J H and Eckstein M 2014 Ultrafast quenching of the exchange interaction in a Mott insulator *Phys. Rev. Lett.* **113** 057201

[39] Mentink J H, Balzer K and Eckstein M 2015 Ultrafast and reversible control of the exchange interaction in Mott insulators *Nat. Commun.* **6** 6708

[40] Hellsvik J, Mentink J H and Lorenzana J 2016 Ultrafast cooling and heating scenarios for the laser-induced phase transition in cuo *Phys. Rev.* B **94** 144435

[41] Anderson P W 1959 New approach to the theory of superexchange interactions *Phys. Rev.* **115** 2–13

[42] Harris A B and Lange R V 1967 Single-particle excitations in narrow energy bands *Phys. Rev.* **157** 295

[43] Chao K A, Spalek J and Oles A M 1977 Kinetic exchange interaction in a narrow *s*-band *J. Phys. C: Solid State Phys.* **10** L271

[44] Takahashi M 1977 Half-filled Hubbard model at low temperature *J. Phys. C: Solid State Phys.* **10** 1289

[45] MacDonald A H, Girvin S M and Yoshioka D 1988 t/U expansion for the Hubbard model *Phys. Rev.* B **37** 9753–6

[46] Peierls R 1933 Zur theorie des diamagnetismus von Leitungselektronen *Z. Phys.* **80** 763–91

[47] Luttinger J M 1951 The effect of a magnetic field on electrons in a periodic potential *Phys. Rev.* **84** 814–7

[48] Aoki H, Tsuji N, Eckstein M, Kollar M, Oka T and Werner P 2014 Nonequilibrium dynamical mean-field theory and its applications *Rev. Mod. Phys.* **86** 779–837

[49] Georges A, Kotliar G, Krauth W and Rozenberg M J 1996 Dynamical mean-field theory of strongly correlated fermion systems and the limit of infinite dimensions *Rev. Mod. Phys.* **68** 13–125

[50] Metzner W and Vollhardt D 1989 Correlated lattice fermions in $d = \infty$ dimensions *Phys. Rev. Lett.* **62** 324–7

[51] Eckstein M and Werner P 2010 Nonequilibrium dynamical mean-field calculations based on the noncrossing approximation and its generalizations *Phys. Rev.* B **82** 115115

[52] Hochbruck M and Lubich C 1997 On Krylov subspace approximations to the matrix exponential operator *SIAM J. Numer. Anal.* **34** 1911–25

[53] Alvermann A and Fehske H 2011 High-order commutator-free exponential time-propagation of driven quantum systems *J. Comput. Phys.* **230** 5930–56

[54] Liechtenstein A, Katsnelson M and Gubanov V 1984 Exchange interactions and spin-wave stiffness in ferromagnetic metals *J. Phys. F: Met. Phys.* **14** L125

[55] Lichtenstein A, Katsnelson M and Gubanov V 1985 Local spin excitations and curie temperature of iron *Solid State Commun.* **54** 327

[56] Liechtenstein A, Katsnelson M, Antropov V and Gubanov V 1987 Local spin density functional approach to the theory of exchange interactions in ferromagnetic metals and alloys *J. Magn. Magn. Mater.* **67** 65

[57] Katsnelson M I and Lichtenstein A I 2000 First-principles calculations of magnetic interactions in correlated systems *Phys. Rev.* B **61** 8906–12

[58] Secchi A, Brener S, Lichtenstein A I and Katsnelson M I 2013 Non-equilibrium magnetic interactions in strongly correlated systems *Ann. Phys.* **333** 221–71

[59] Floquet G 1883 *Ann. Sci. Norm. Super.* **12** 47–88

[60] Grifoni M and Hänggi P 1998 *Phys. Rep.* **304** 229–354

[61] Itin A P and Katsnelson M I 2015 Effective hamiltonians for rapidly driven many-body lattice systems: induced exchange interactions and density-dependent hoppings *Phys. Rev. Lett.* **115** 075301

[62] Bukov M, Kolodrubetz M and Polkovnikov A 2016 Schrieffer-wolff transformation for periodically driven systems: strongly correlated systems with artificial gauge fields *Phys. Rev. Lett.* **116** 125301

[63] Kitamura S and Aoki H 2016 η-pairing superfluid in periodically-driven fermionic Hubbard model with strong attraction *Phys. Rev.* B **94** 174503

[64] Elliott R and Loudon R 1963 The possible observation of electronic raman transitions in crystals *Phys. Lett.* **3** 189–91

[65] Fleury P A and Loudon R 1968 Scattering of light by one- and two-magnon excitations *Phys. Rev.* **166** 514

[66] Shastry B S and Shraiman B I 1990 Theory of raman scattering in Mott-Hubbard systems *Phys. Rev. Lett.* **65** 1068–71

[67] Lorenzana J and Sawatzky G A 1995 Theory of phonon-assisted multimagnon optical absorption and bimagnon states in quantum antiferromagnets *Phys. Rev.* B **52** 9576–89

[68] Devereaux T P and Hackl R 2007 Inelastic light scattering from correlated electrons *Rev. Mod. Phys.* **79** 175–233

[69] D'Alessio L and Rigol M 2014 Long-time behavior of isolated periodically driven interacting lattice systems *Phys. Rev. X* **4** 041048

[70] Lazarides A, Das A and Moessner R 2014 Equilibrium states of generic quantum systems subject to periodic driving *Phys. Rev. E* **90** 012110

[71] Zhao J, Bragas A V, Lockwood D J and Merlin R 2004 Magnon squeezing in an antiferromagnet: reducing the spin noise below the standard quantum limit *Phys. Rev. Lett.* **93** 107203

[72] Zhao J, Bragas A V, Merlin R and Lockwood D J 2006 Magnon squeezing in antiferromagnetic MnF_2 and FeF_2 *Phys. Rev.* B **73** 184434

[73] Kalashnikova A M, Kimel A V, Pisarev R V, Gridnev V N, Kirilyuk A and Rasing T 2007 Impulsive generation of coherent magnons by linearly polarized light in the easy-plane antiferromagnet $FeBo_3$ *Phys. Rev. Lett.* **99** 167205

[74] Mikhaylovskiy R V, Huisman T J, Popov A I, Zvezdin A K, Rasing T, Pisarev R V and Kimel A V 2015 Terahertz magnetization dynamics induced by femtosecond resonant pumping of Dy^{3+} subsystem in the multisublattice antiferromagnet $DyFeO_3$ *Phys. Rev.* B **92** 094437

[75] Mikhaylovskiy R, Huisman T J, Pisarev R V, Rasing T and Kimel A V 2017 Selective excitation of terahertz magnetic and electric dipoles in Er^{3+} ions by femtosecond laser pulses in $ErFeO_3$ *Phys. Rev. Lett.* **118** 017205

[76] Evans R F L, Fan W J, Chureemart P, Ostler T, Ellis M and Chantrell R 2014 Atomistic spin model simulations of magnetic nanomaterials *J. Phys.: Condens. Matter* **26** 103202

[77] Eriksson O, Bergman A, Bergqvist L and Hellsvik J 2017 *Atomistic Spin Dynamics* (Oxford: Oxford University Press)

[78] Hellsvik J *et al* 2014 Tuning order-by-disorder multiferroicity in cuo by doping *Phys. Rev.* B **90** 014437

[79] Johnson S L *et al* 2012 Femtosecond dynamics of the collinear-to-spiral antiferromagnetic phase transition in cuo *Phys. Rev. Lett.* **108** 037203

[80] Stevens T E, Kuhl J and Merlin R 2002 Coherent phonon generation and the two stimulated raman tensors *Phys. Rev.* B **65** 144304

[81] Kittel C 1963 *Quantum Theory of Solids* (New York: Wiley)

[82] Fazekas P 1999 *Lecture Notes on Electron Correlation and Magnetism* (Singapore: World Scientific)

[83] Feynman R P, Vernon F L Jr and Hellwarth R W 1957 Geometrical representation of the schrödinger equation for solving maser problems *J. Appl. Phys.* **28** 49–52

[84] Gridnev V N 2008 Phenomenological theory for coherent magnon generation through impulsive stimulated raman scattering *Phys. Rev.* B **77** 094426

[85] Claassen M, Jiang H C, Moritz B and Devereaux T P 2016 Dynamical time-reversal symmetry breaking and photo-induced chiral spin liquids in frustrated Mott insulators (http://arxiv.org/abs/1611.07964)

[86] Stepanov E A, Dutreix C and Katsnelson M I 2017 Dynamical and reversible control of topological spin textures *Phys. Rev. Lett.* **118** 157201

[87] Kitamura S, Oka T and Aoki H 2017 Probing and controlling spin chirality in Mott insulators by circularly polarized laser *Phys. Rev.* B **96** 014406

[88] Gavrichkov V A, Polukeev S I and Ovchinnikov S G 2017 Contribution from optically excited many-electron states to the superexchange interaction in Mott-Hubbard insulators *Phys. Rev.* B **95** 144424

[89] Eckstein M, Mentink J H and Werner P 2017 Designing spin and orbital exchange hamiltonians with ultrashort electric field transients (http://arxiv.org/abs/1703.03269)

[90] Meyer U, Haack G, Groth C and Waintal X 2017 Control of the oscillatory interlayer exchange interaction with terahertz radiation *Phys. Rev. Lett.* **118** 097701

[91] Kampfrath T, Sell A, Klatt G, Pashkin A, Mährlein S, Dekorsy T, Wolf M, Fiebig M, Leitenstorfer A and Huber R 2010 Coherent terahertz control of antiferromagnetic spin waves *Nat. Photon.* **5** 31

[92] Baierl S, Hohenleutner M, Kampfrath T, Zvezdin A K, Kimel A V, Huber R and Mikhaylovskiy R V 2016 Nonlinear spin control by terahertz-driven anisotropy fields *Nat. Photon.* **10** 715–18

[93] Baierl S *et al* 2016 Terahertz-driven nonlinear spin response of antiferromagnetic nickel oxide *Phys. Rev. Lett.* **117** 197201

[94] Sato M, Takayoshi S and Oka T 2016 Laser-Driven Multiferroics and Ultrafast Spin Current Generation *Phys. Rev. Lett.* **117** 147202

[95] Brück E, Tegus O, Thanh D and Buschow K 2007 Magnetocaloric refrigeration near room temperature (invited) *J. Magn. Magn. Mater.* **310** 2793–9 (Proc. of the 17th Int. Conf. on Magnetism)